Numerical Methods in Civil Engineering, 6-3 (2022) 78-91

Numerical Methods in Civil Engineering

Journal Homepage: https://nmce.kntu.ac.ir/

Experimental and finite element study of one span concrete bridge bent designed by the requirements of the 1970s, under gravity and lateral load

Mohammad Kazem Bahrani [*], Amin Nooralizadeh [**], Mahdy Sharify [***], Najmeh Karami [****]

ARTICLE INFO

RESEARCH PAPER

Article history:
Received:
July 2021.
Revised:
September 2021.
Accepted:
October 2021.

Keywords:
Concrete Bridge Bent
Finite Element Model
Reinforcement
Absorbed Energy
failure

Abstract:

In recent years, there has been a growing seismic demand for existing bridges and the final redesign of bridges, especially after a major earthquake One method to strengthen concrete frames on bridges is to use steel sheets or profiles to use the confining force. During this study, a sample at 30% scale under gravity and lateral cycle loading was examined within the laboratory. A finite element model is additionally used to compare the behavior of laboratory samples. The laboratory sample was a model of a typical bridge in iran that was generally designed with deficient detailing requirements in agreement with the typical regulations of the 1970s. A finite element analysis set was used to evaluate various parameters in improving the behavior of the laboratory sample. The finite element model correctly predicted the weakness of the model. Subsequently, a reinforced specimen was investigated by increasing the prestressing force within the concrete beam and the thickness of the frp sheets utilized in the bridge pier by the finite element method. The results show the energy absorbed within the hysteresis curves improved the propagation of the failure. The result also showed that a 100% increase in the prestressing load caused a 67% increase in resistance .

1. Introduction

Because many bridges are located in seismic areas, they may suffer irreparable damage or even collapse when exposed to strong earthquakes [1]. Bridge damage is usually caused by superstructure movement, joint failure, bent damage of the column due to shear or flexure, and abutment failure [5-2]. Therefore, bridges located in seismic areas need seismic reinforcement to be prevented from damage in severe earthquakes and to maintain their services after the earthquake. As demonstrated by the 2011 Tohoku earthquake, repaired bridges perform better in many earthquakes. Therefore, bridge reinforcement is very important [3] and can affect vital transportation operations after the earthquake [6].

Also, in cases where the bridge design follows the old codes, proper seismic reinforcement is required to bring the failure states closer to the desired states, by creating a weak column–strong beam using the principles of seismic design. [7-8]. The study of seismic reinforcement of bridges is of interest to many researchers and information about samples and their characteristics is easily available from experiments in research centres [9]. So far, various methods of reinforcement have been investigated, such as the use of fiber-reinforced plastic cover (FRP) [10], the creation of concrete cover around the sections [7], the removal of the connection zone of the cap beam–column [7], Increase of shear rebars in the joint [7], and other methods used to reduce the seismic demand in the column [11]. The first and most serious study on this subject was the experimental tests of Priestley theory [12-13] which examined the effect of a steel cover installed on the whole column in increasing the shear strength of concrete columns of the bridge frame. Due to the high cost of reinforcing the entire height of the column with a steel cover and the high time cost, this method currently seems incompatible. Some studies have also been

* *Corresponding author: Assistant professor, Department of Civil Engineering, University of Qom, Qom, Iran. Email: mkbahrani@ut.ac.ir.*
** *PhD candidate , Department of Civil Engineering, University of Qom, Qom, Iran.*
*** *Assistant professor, Department of Civil Engineering, University of Qom, Qom, Iran.*
**** *PhD student, Department of Civil Engineering, University of Qom, Qom, Iran*

made on the reinforcement of composite materials, such as carbon fiber reinforced polymers (CFRPs), which are installed on bridge piers. In one study, it was shown that in such case, the shear strength of joint ductility and displacement increases significantly. Given that FRP materials cover a large area of beams and columns, it is both costly and time consuming, and therefore not feasible. Other reinforcement methods have been studied by researchers, such as reinforcement of a straight reinforced concrete bridge with non-buckling braces (BRB) to increase the strength of foundations under seismic loads, reduce displacement and increase seismic resistance under post-earthquake service conditions [1] This method of retrofitting has also been studied by other researchers. The Priestley et al. (1993) retrofit plan for a two-story San Francisco bridge was used only for the cap beam–column connection zone and in cases where the column of the cap beam of the bridge was weak. However, this method encountered problems that included the difficulty of shuttering and concreting in the small area on the joint region, and in high regions, creating the required bonding between the new and old concrete, and completing the intricate details of reinforcing.

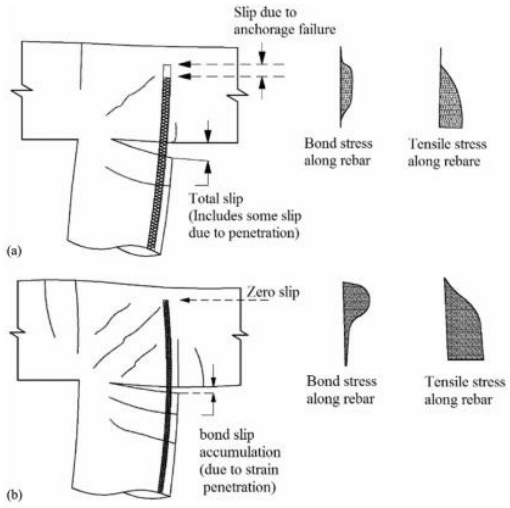

Fig. 1: Slip of longitudinal bars in the connection zone of reinforced concrete frame: (a) Slip of the joint due to insufficient anchorage of longitudinal bars; (b) Slip due to strain penetration

Prestressing was introduced by Sitran et al. [14] due to its major benefits such as increased shear strength, reduced surface tension due to shear in the joint and increased flexural capacity of the cap beam. However, it is impossible to ignore the main disadvantages of prestressing: reduced ductility and embrittlement of the member due to significant axial forces. In terms of reinforcement of existing structures, there are setbacks in execution. The reinforcement technique of Pantlides et al. [15] is also an effective technique for strengthening the piers of bridges in which the foundation lacks sufficient rigidity and strength. Accordingly, a horizontal reinforcement strand can be created at the top of the foundation and at the level of the cap beam. This is good for new bridges, but in terms of reinforcing existing bridges, it can cause the problems mentioned above, especially in the area of the concrete column connection. Mander and Chen [16] reinforcement technique can be considered as a good, efficient and successful technique. The frame failure mechanism was successfully modified to a desirable mechanism, and it was found that this method was quite successful if the shear weakness of the columns did not dominate the final strength. The setbacks of this reinforcement design are due to insufficient anchorage of longitudinal rebars and defects in the shear strength of the columns, which can be amended easily without the intervention of other members. In the reinforcement design of a bridge frame containing a pile, the columns were weakened and the beams and joints were strengthened. The purpose of this project was to modify the failure mechanism and increase ductility, which was successful in the first attempt, but failed in the succeeding endeavor due to the severe weakness of the connection area.

One of the reasons for the decrease in strength and undesirable seismic behavior in the concrete frame of the bridges is insufficient anchorage of longitudinal rebars used in the connection area. This issue should be considered in choosing the appropriate retrofitting technique, and one of the goals of the retrofitting design should be to strengthen the connection area properly and purposefully as slipping rebars in RC structures often occur at this location.

One of the major problems of these bridges is the weakness in the cap beam–column connection. This weakness is due to insufficient transverse rebars in the joint connection, which leads to slippage of rebars under seismic loads in this area [7]. In this study, a sample was studied experimentally and compared with a finite element model (FEM). This model was built according to the average conditions of the built bridges, which were designed based on the old version of the bridge design specifications [18]. At that time, there were no seismic design criteria in Iran and the bridges were designed for gravity loads.

These bridges are usually supported by multiple columns and have a simple span or continuous concrete deck mounted on a beam. These frames are usually characterized by strong columns and weak beams, with some defects in detail and confinement, especially in the joints [19]. Prominent prestressed concrete bridges are widely used due to their excellent properties, such as low price and beautiful appearance [20 - 29]. Vertical tensile stress is considered as the main cause of failure [30, 31]. Pan et al. [32] conducted a field study and divided these cracks into two main groups: longitudinal cracks and flange base cracks. Magley et al. [27] have developed the scaling process as the third type of

cracking. Podolny et al. [25] present four types of cracking at the bottom. Further analysis of the response of the structural system of prefabricated component steps is required to change the load that occurs during the fabrication sequence [33]. Structural performance in the thin-walled cubic structure is very complex and several two-dimensional analyses have been used for structural design [34-36]. According to the applicable regulations [37, 38], the transverse effects are ignored because the effect of the pre-stretched strands is mainly on the bottom. Theoretical simulation of bottom plate failure during prestressing is complex. Accurate and efficient modelling of prestressing effect as well as nonlinear failure process analysis is desirable [39, 40].

Cracking is common in reinforced concrete (RC) bridges and other structures, but is not necessarily harmful. Many structures are designed to break under service loads. However, cracking needs to be controlled to ensure durability and aesthetic needs. Current regulations set limits on crack width and minimum reinforcement level. The causes of cracking in concrete members are many. Cracks may occur in concrete structures due to internal or external restraints. For example, temperature changes between different parts of a structure can change the nature of different needs. If those deformations are prevented, it may crack [41], [42]. In practice, however, some cracks may cross the specified boundaries, even if design regulations are followed. Most importantly, cracking not only negatively affects the durability and aesthetics, but may also affect the ductility and structural capacity of an RC member. It has been experimentally shown that the effect on ductility and final capacity can be positive or negative, depending on the location and characteristics of the crack as well as the state of failure. Cracks should be included in the structural assessment to consider their impact on ductility, capacity and failure condition, and therefore, there is a need for improved assessment of reinforced concrete infrastructure.

One way to improve evaluation is to include up-to-date information about the structure, for example, information about pre-existing cracks. This may be facilitated by Digital Twin (DT) models, which in the future are expected to play a vital role in the optimal management of critical infrastructure [43]. DT is a virtual copy of the structure which saves information collected over the life of the structure (for example, through various types of sensors). It may provide insight into structural capacity through finite element analysis (FE). It may also act as a decision support tool [44,45].

2. Laboratory Sample Description

The design of the laboratory sample was based on field studies, the indicated specifications for the structure of the base frame, the scope of the study and the available facilities. Figure 2 shows the laboratory specifications of the fabricated sample. The sample made in the 1370s was designed to show real samples common in Iran. In the construction of the samples, the ratios of the cross-sectional areas of the longitudinal and transverse bars and the dimensions of the sections and openings are similar to the average values in the studied steps. For example, the details of the longitudinal rebars of the columns are listed in Table 1.

The conventional design method at the time of construction of these bridges does not dictate the control of the relative flexural capacity of the column cap by considering the shear force transfer from the joint. Figure 2 shows the geometric dimensions of the constructed sample.

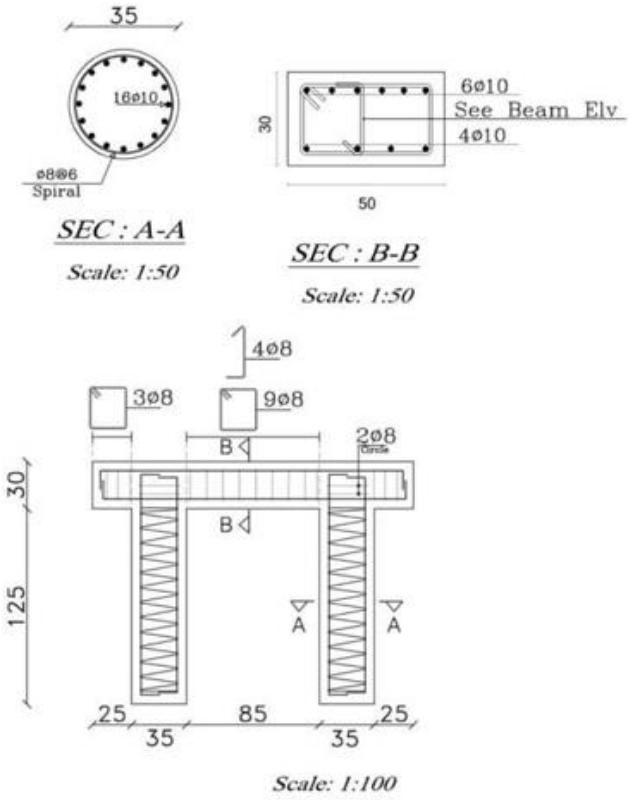

Fig. 2: Built-in sample Detail

Due to the size of laboratory facilities, available size and dimensions, jack capacity, frame limitations, the possibility of placing samples and gravity and lateral loads was not possible This test was performed in the structural laboratory of the University of Tehran.

Table 1: Mechanical specifications of longitudinal and transverse bars of columns

Ultimate strain (%)	Ultimate stress (MPa)	Yield stress (MPa)	Rebar type
12.56	653.2	511.4	Longitudinal
12.34	540.8	365.4	Transverse

For concrete, the sample strength of standard cylinders was considered to be approximately 40 MPa. The compressive strength of concrete in the samples is given in Table 2. Also, longitudinal rebars of type AIII with yield stress of 511 MPa and transverse bars of type AII with yield stress of 365 MPa were selected. The concrete mix design was prepared for optimum strength, except that the diameter of the largest aggregate was reduced to 15 mm. The number and details of the longitudinal columns of the column are exactly the same as the existing rebars with full symmetry of the column cross section.

Table 2: Compressive strength of concrete

Compressive strength of concrete (MPa)	Member
41.6	Cap beam
40.7	column

As mentioned, the main problems of the studied structures are anchorage of longitudinal rebars in the joint area, which causes significant damage in the joint zone and the cap beam and reduces the energy absorption and loss capacity. The longitudinal rebars of the columns should be limited at the connection zone with the transverse bars. Failure to execute details or incomplete execution will cause damage to the frames under study. Confining force can be provided by transverse cross members, diaphragms, or transverse bars. In the studied frame, concrete confinement was applied by applying prestressing force to the connection zone of the longitudinal rebars from the outside. Figure 2 shows the details of the sample and the retrofitting method is described below.

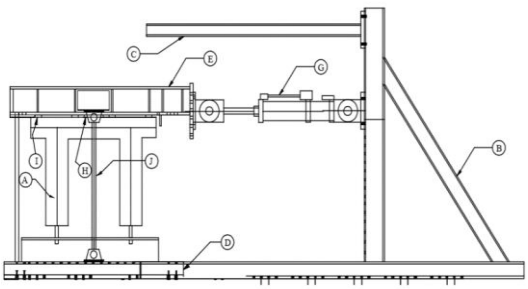

Fig. 3: Schematic of setting up a laboratory sample

Figure 3 shows a schematic of the test instrument, parts and components used to set the laboratory sample and create a rigid floor. These are also explained in the discussion below. One of the bases in the laboratory was used for rigid support and lateral loading.

Fig. 4: Setting up laboratory sample

Gravity load was applied by the use of eight bolts that were prototyped symmetrically on both sides of the laboratory specimen (Figure 3, Section E). The required gravity load was applied to the frame by attaching one side of the cross beam to the jack and the other side to the tensile element, which moved freely along both sides of the specimen during the test. An axial load of 200 kN was constantly applied to the sample during test. By placing the steel shear keys at the connection zone of the cross beam and the specimen, the actual conditions and the application of lateral force in the laboratory model were applied. Loading was applied to the transverse beam with a horizontal reciprocating jack. The height of the jack position was adjusted in such a way that the actual level of the bridge deck mass and the region of the effect of the jack's force had the necessary compliance.

The yield displacement of 24 mm was estimated based on the initial analysis and observations during the experiment in accordance with the initial software model with SAP2000 and was considered as a criterion for applying lateral load. Loading was continued until a loss of strength was observed, ensuring that the frame reached its maximum capacity. The loading protocol is shown in Figure 5.

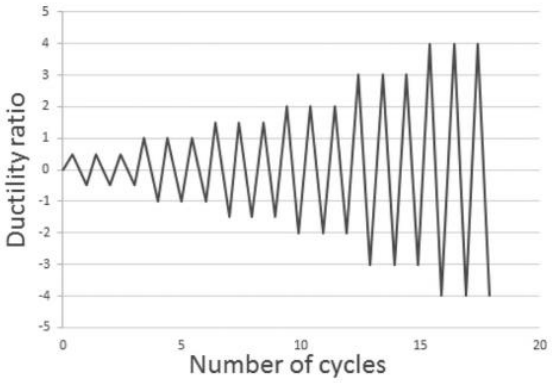

Fig. 5: Loading protocol

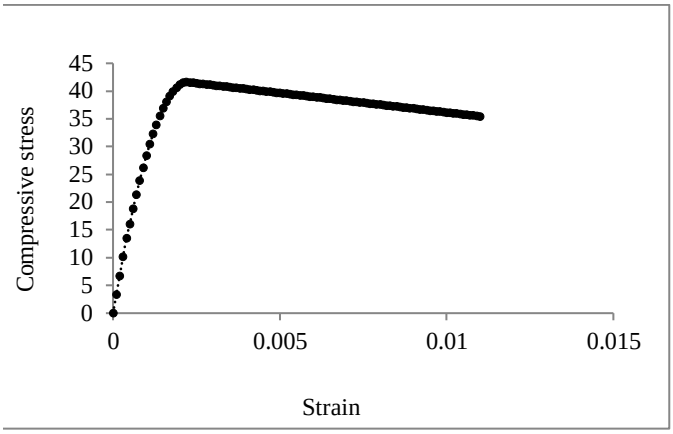

Fig. 6: Stress-strain curve for concrete with a compressive strength of 41.6 MPa

3. Finite element modeling

The concrete diagram in pressure is determined based on the results of uniaxial concrete compression test. For concrete in pressure, three areas of the diagram are introduced. The first part of the diagram is assumed to be elastic to some extent proportional to that stress. The value of this stress is considered equal to $0.4\ f_c$. Where f_c is the compressive strength of concrete. Strain ε_1 is related to stress equal to 0.0022. The Young's modulus is also calculated on the basis of the Poisson's ratio equal to 0.2. The second part of the diagram, which has a parabolic shape, starts from a point with a limit stress and continues until it reaches the highest compressive strength of concrete. This part of the graph is determined by Equation (1):

$$\sigma_c = \left(\frac{kn - n^2}{1 + (k-2)n} \right) f_{ck} \quad (1)$$

$$n = \frac{\varepsilon_c}{\varepsilon_{c1}} \quad (2)$$

$$\varepsilon_{c1} = 0.0022$$

$$k = 1.1 E_{cm} \times \frac{\varepsilon_{c1}}{f_{ck}} \quad (3)$$

Where E_{cm} is the modulus of elasticity of concrete.

The third part of the stress-strain curve is the descending part of the graph from f_c to rf_c, in which the reduction factor, r is considered to be 0.85.

The final strain of concrete, ε_{cu} is equal to 0.01.

In software, the stress-strain curve must be introduced as the corresponding inelastic stress-strain. Inelastic strain is equal to the difference between total strain and elastic strain. The relationship between total, inelastic and elastic strains is as follows:

$$\varepsilon_{el} = \frac{\sigma_t}{E} \quad (4)$$

$$\varepsilon_{in} = \varepsilon_t - \varepsilon_{el} \quad (5)$$

In the above relations, ε_t is the total strain, ε_{el} is elastic strain and ε_{in} is considered as the plastic strain.

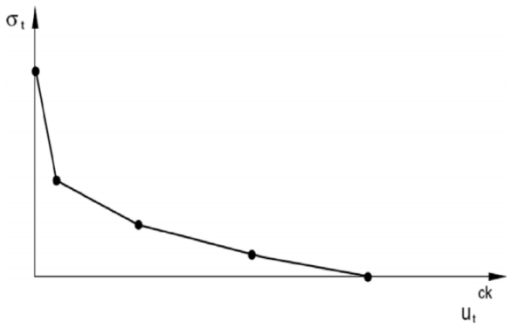

Fig. 7: Concrete behavior based on tensile stress (cracking of concrete) [46]

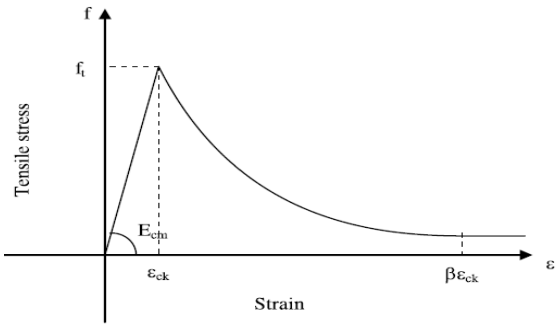

Fig. 8: Behavior of concrete in tension[46]

The gradual decrease in stiffness can be characterized in two ways, either by a stress-strain relationship after the crack point or by applying a crack energy rupture criterion shown in the figure. In the software guide, it is suggested that in cases where concrete reinforcement is not suitable, it is better to replace the brittle behavior of concrete in the form of rupture energy with a stress-strain relationship for the tensile behavior of concrete.

Tensile damage parameter was also used in modeling the behavior of concrete materials. The elastic stiffness of concrete materials decreases after the concrete cracks. The reduction in elastic stiffness is determined by two damage parameters, which are considered as a function of plastic strain. These parameters can take values from zero to 1, the value of zero indicates a state that has not suffered any failure, and the value of 1 indicates a state where all strength is lost. In the tests, it was observed that the concrete cracked in the joint area, but no corrosion of the concrete occurred in the upper and lower part of the joint. Therefore, in the finite element modeling, only the tensile failure parameter is applied (Figures 7 and 8).

Taking C40 grade concrete as an example to calculate the damage factor, the material properties are: uniaxial compressive strength characteristic value f_{ck} =26.8N/mm^2 f , uniaxial tensile strength characteristic value f_{tk} =26.8N/mm^2, elastic modulus E_0 =2.739310^4 N/mm^2, Poisson's ratio =0.2 , dilation angle ψ =30 , eccentricity = 0.1 , the ratio of initial equibiaxial compressive yield stress to initial uniaxial compressive yield stress is f_{b0} / f_{c0}=1.16 , the ratio of the second stress invariant on the tensile meridian to that on the compressive meridian K_c=0.6667 , viscosity parameter μ=0.0001.

ABAQUS modelling must be performed using true stress and true strain. Thus, the equations for converting engineering stress to true stress are used as follows (Eqs. 4-5):

$$\overline{\sigma} = \sigma(1 + \varepsilon) \quad (4)$$

$$\overline{\varepsilon} = ln(1 + \varepsilon) - \sigma/E \quad (5)$$

Where E is elastic modulus, σ is engineering stress, ε is engineering strain, $\overline{\sigma}$ is true stress and $\overline{\varepsilon}$ is true strain and figure. 2 illustrates the values of yield and ultimate stress as F_y is 360 MPa and Fu is 506 MPa.

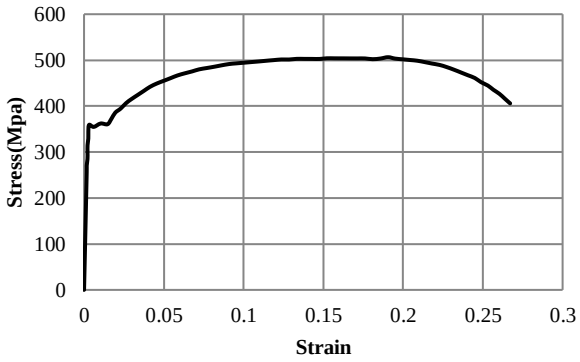

Fig. 9: Engineering Stress-Strain Curve

Converting equations can only be used to calculate the true stress before the necking stage, after which stress and strain would be concentrated on a particular point. On the other hand, the stress-strain curve must cover the range of strain up to 0.9 in order to depict the fracture. Hence, the below equation is proposed in Eq.6.

$$\sigma = K\varepsilon^m \quad (6)$$

Based on the diagram, the values of m and K are equal to 0.195 and 841.34 respectively. As these factors are obtained, the true stress-strain curve would be as figure 10.

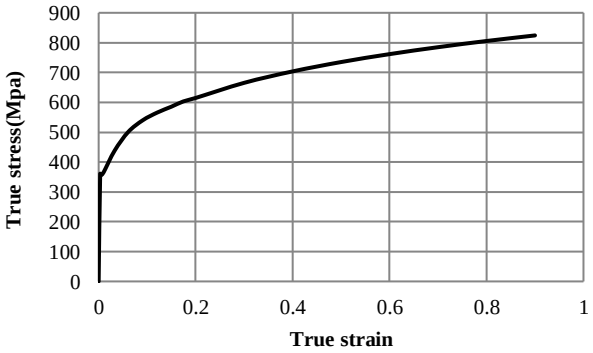

Fig. 10: True Stress-Strain Curve

3.1 Modeling of components

For all samples, the model geometry, including components such as concrete columns, concrete beams, reinforcements and rigid supports, and loading in the software, were modeled separately as shown in the figure, and finally attached together. These components were made entirely in software. Since constraints and interactions between components have a great impact on the results of the analysis, an effort was made to apply them accurately and in accordance with the experiment (Figure 11).

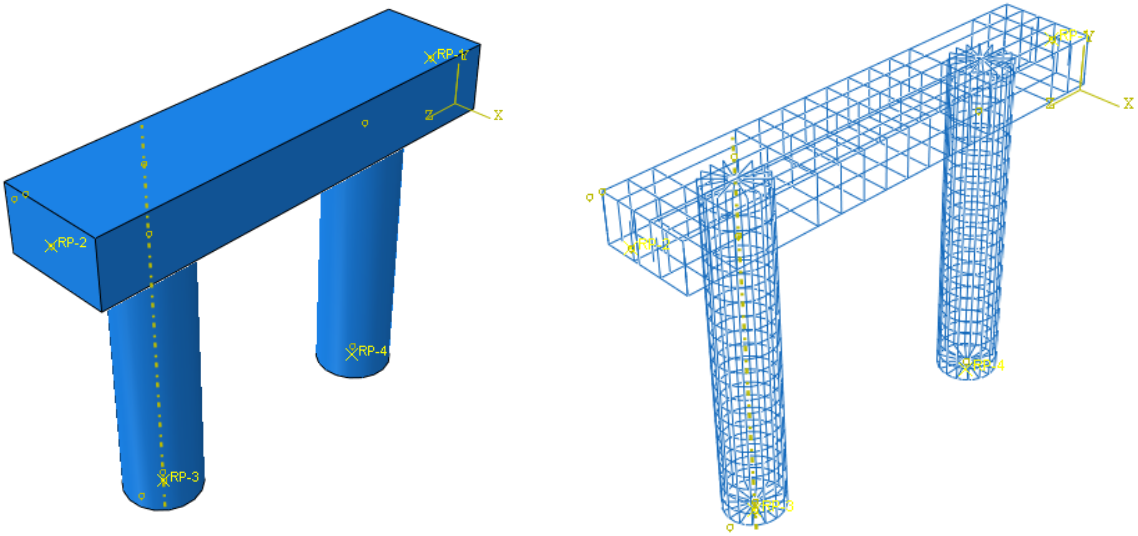

Fig. 11: 3D model in finite element analysis (right side, reinforcements and left side, columns and concrete beams)

3.2 Type And Size of Elements

Concrete columns are modeled by the three-dimensional elements available in the ABAQUS software library, which are essentially the 8-point elements used for nonlinear analysis involving surface to surface contact, large deformations, plasticity, and failure. Concrete beams and other components were also meshed with C3D8R elements as shown in Figure 10. The reinforcements were also modeled by T3D2 truss elements. Also, to reduce the analysis time, elements with larger sizes were used in most parts and smaller elements were used in the areas of the connection zone (Figure 12).

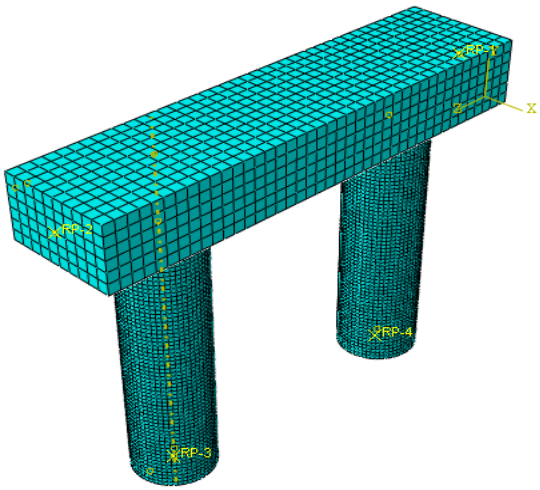

Fig. 12: Finite element model mesh

3.3 Interaction And Conditions Of Constraints Between Different Components

To assemble the concrete beam with the concrete column, the tie constraint , which fixed all the degrees of freedom of the upper and lower plates of the concrete column and the end plates of the beam, was used. For rigid plates, a reference point was defined, where all degrees of freedom of these plates are affected by this point, called the reference point. While defining a tie constraint, two surfaces are tied together, in which, one of them is defined as a master and the other as a slave. As mentioned in the software guide, to avoid numerical errors, it is better that the slave level corresponds to a surface whose materials are softer and the dimensions of its elements are smaller than the master surface. Therefore, when this constraint is used, the displacement of the Slave surface points is obtained by the displacement of the Master surface points, and in fact the relative slip between these two levels is ignored. To place the reinforcements in the concrete, the Embedded constraint was used, in which the degrees of transfer freedom of the nodes in the elements of the reinforcement are limited to the degrees of freedom of the corresponding nodes in the concrete elements and the slip of the reinforcements in the concrete is considered zero.

3.4 Boundary conditions

In laboratory tests, the concrete column is in accordance with the test and its connection is pinned to the foundation. Therefore, in its software modeling , all degrees of transitional freedom are closed and the rotation of the column end, which is connected to the rigid support plate, is

released. In fact, this boundary condition is applied to the reference point of the rigid plane, which is affected by the movement of other nodes (Figure 13). The displacement and gravity force applied to the finite element model are also shown in Figure 14.

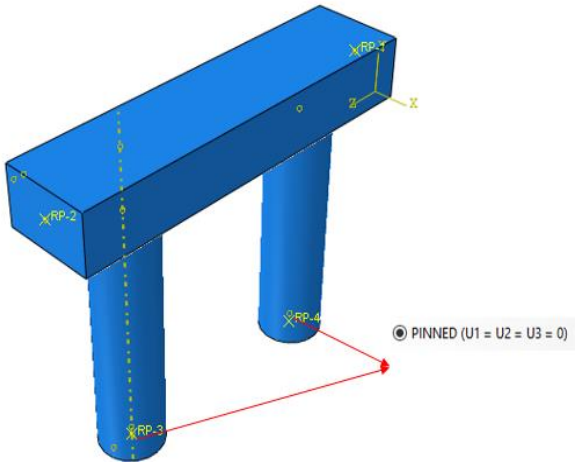

Fig. 13: Boundary conditions of the columns

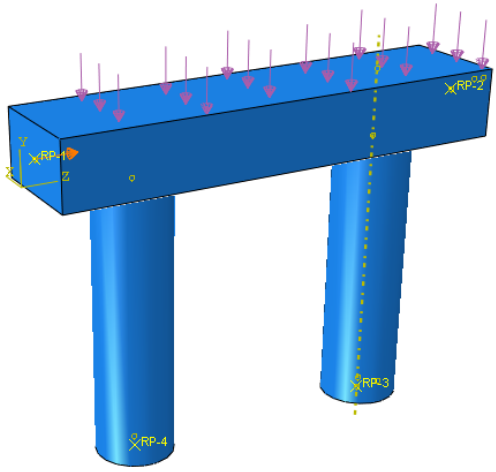

Fig. 14: Displacement applied to the end of the beam and axial load uniformly applied to the top of the concrete beam in FE model

4. Comparing finite element analysis and laboratory results

The behavior of the concrete frame in the experimental model is compared with the numerical model. Cyclic loading was applied to the concrete beam to bring the sample to yield (rebar fracture and concrete cracking). The behavior of the concrete frame as well as the curves obtained are compared with the results of the numerical model. Figures 15 and 16 show the hysteresis curves of the numerical and laboratory models of the samples.

At the beginning of the work, to ensure that the sample was properly modeled and the assumed parameters had reasonable values, the finite element sample of the laboratory sample was checked and it was observed that the finite element analysis results and the laboratory results were in good agreement. And then a parametric study was conducted to investigate how the various components of the connection are affected.

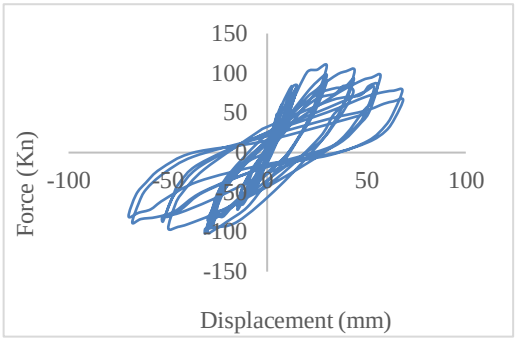

Fig. 15: Force - displacement diagram of beam in laboratory model

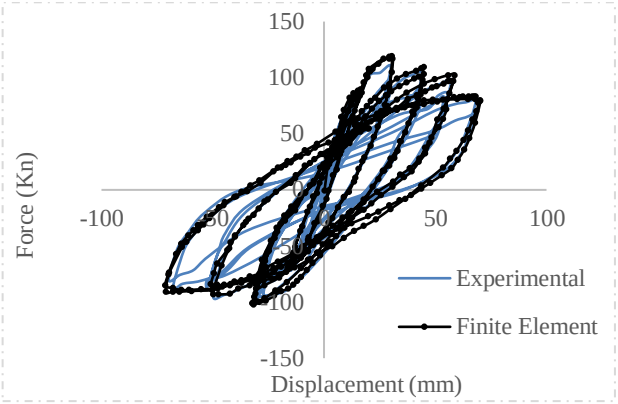

Fig. 16: Comparison of force-displacement diagrams of beam in FE model and laboratory model

As it is known, the results of numerical analysis and laboratory results are consistent with each other and show exactly the same behavior and experience maximum strength in displacement of approximately 24 mm, but in displacements higher than this value, due to cracking of concrete in the finite element the model has decreased in strength. The only difference between the two diagrams is that in the finite element model, due to the non-slip of reinforcements in concrete, the phenomenon of pinching is not seen in the finite element diagram. But in terms of strength, they are reasonably compatible with each other. Therefore, with the relevant details, the numerical model can be easily applied in similar cases. To accurately study the

seismic parameters and the impact of retrofitting, some important parameters were calculated, as discussed in the following section.

4.1 Cracks in concrete columns and beams

In this experiment, displacement is applied to the cap beam by a hydraulic actuator, and the column is allowed to rotate within the plate at one end and is attached to the beam at the other end. As can be seen from Figure 17, cracks in the concrete column start from the connection point to the concrete beam near the load region and gradually spread to the lower area of the column as the load continues. It is also clear that due to double curvature in concrete beams, cracks spread from the bottom to the top of the concrete beam at the point of connection to the concrete column near the place of application of the load and at the point of connection to the next concrete column. The loading of this process will also be reversed, so in the lateral loading, the places that need reinforcement are the connection of the column to the column beam, as well as the areas of the concrete beam that are adjacent to the column. Another important point is that the cracks that form on the surface of the concrete column do not spread perpendicular to the outer surface of the concrete and will spread with a gentle slope towards the joint. This point is important because if the concrete column needs to be reinforced, the rebars that will be placed in this area can be placed perpendicular to the direction of cracking, the best case of which is the placement of the arch perpendicular to the crack path. As it is known, the cracks in the joint area in the laboratory model and the finite element model are well matched with each other and correctly predict the cracking behavior in the case. Therefore, by recognition of the crack path as well as the areas prone to cracking, different reinforcement methods can be used to delay the onset of cracking and also increase the strength of the reinforcement method, which will be mentioned in this article. The fibers are FRP. Prestressing is used to prevent cracking of concrete beams and FRP fibers are used to delay column cracking. The following figure shows the amplified regions in the finite element model (Figure 18).

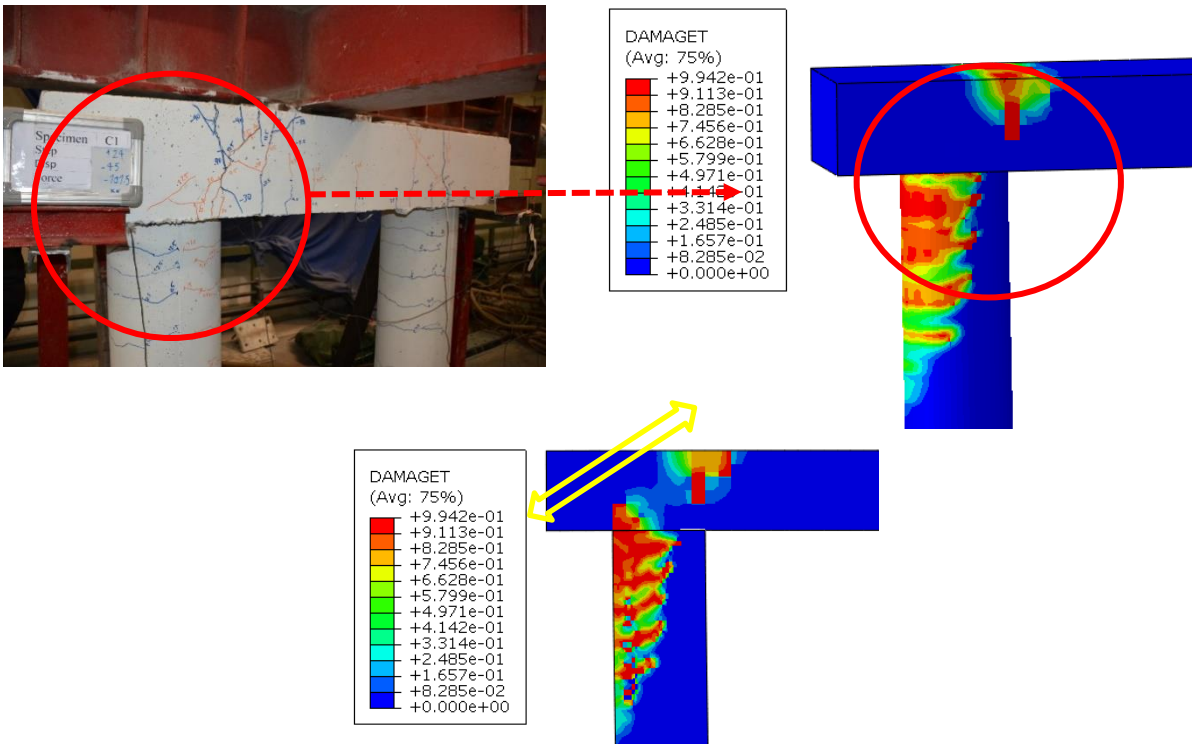

Fig. 17: Comparison of cracking in FE model and laboratory model

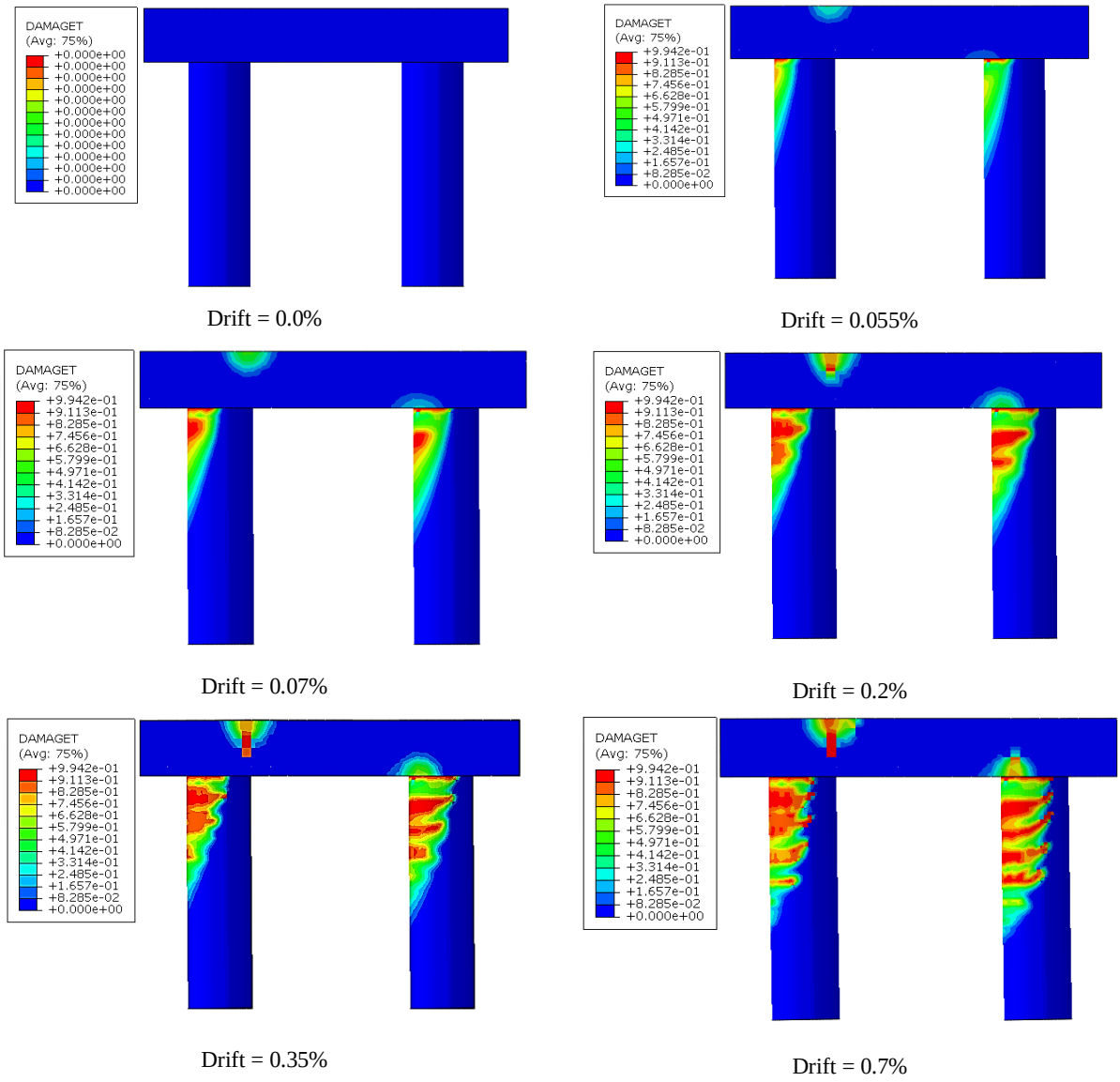

Fig. 18: The propagation of diagonal cracks in the connection zone in the finite element model

4.2 Minimum and maximum main stress distributions

Figure 19 shows the formation of stresses in the rebars, according to which the concentration of stress in the rebars of the columns in the joint area and below indicates that the reinforcements in this area are strongly under tension due to loading, as well as cracks in the concrete beam shown in the previous figures are also the location of the maximum stresses of the longitudinal beams embedded in the concrete beam. Figure 20 also shows the main maximum and minimum stresses, which are mainly shown with red and blue arrows. It is clear according to the direction of the arrows, corrosion has started to expand, and if necessary, more attention can be paid to reinforcement of these areas.

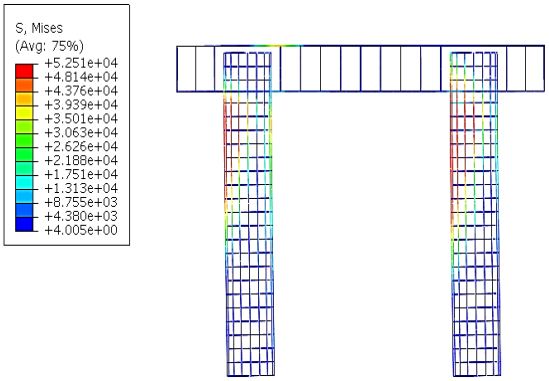

Fig. 19: Mises stresses formed in steel reinforcements

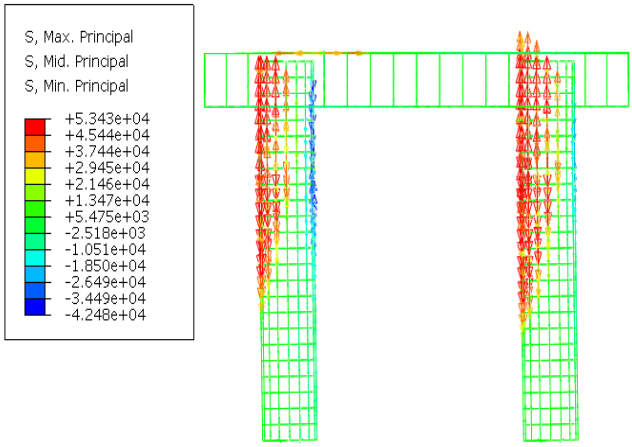

Fig. 20: Minimum and maximum main stresses formed in reinforcements

Figure 21 shows how to create the main strains in steel components, which according to the contour of the strains and also the direction of the arrows in the figure can identify in which areas most strains will be in the rebars.

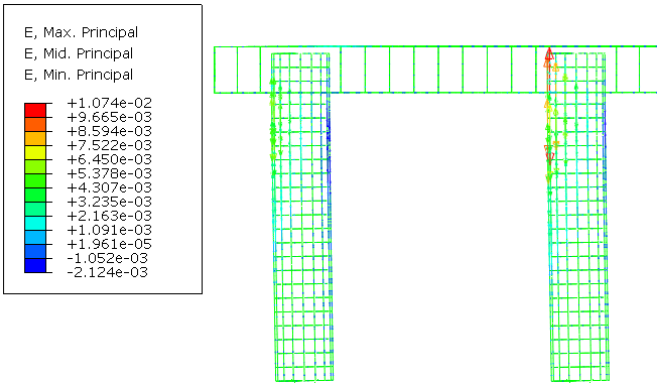

Fig. 21: Minimum and maximum main strains in reinforcements

4.3 Strengthening of the finite element model

By recognizing the areas prone to cracking and creating a plastic joint, the sample can be strengthened. As it is known, the reinforced sample includes prestressing in the concrete beam section, which in finite element software is done as a compressive load on both sides of the beam before horizontal displacement. In the lower part, where the concrete columns are located, FRP, which is covered with half of the column length, was used to delay cracking in the column. As it is clear from the results, this reinforcement method has increased the final strength and ductility by calculating the area under the displacement force curve (Figure 22).

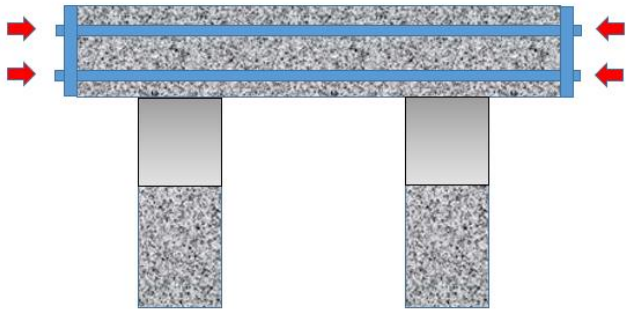

Fig. 22: Schematic of finite element model strengthening

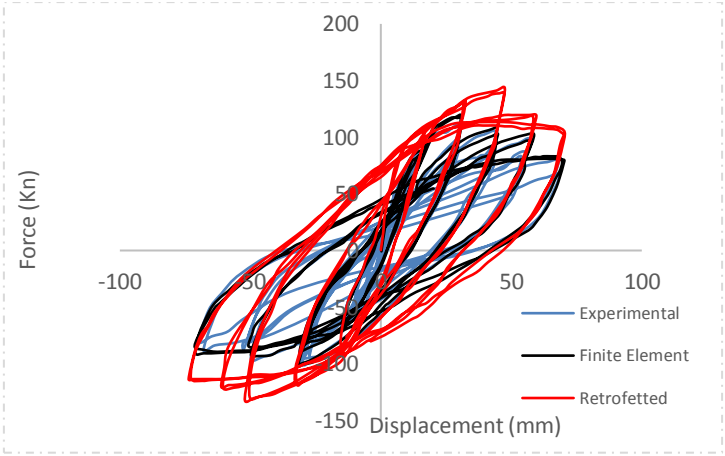

Fig. 23: Comparison of force displacement diagrams of beam in FE model and laboratory model and retrofitted finite element model

Improvements in the seismic behavior of the reinforced specimen were significant compared to the fabricated specimen. For example, since the specimens are loaded to their final capacity, the increased capacity and the area under the pressure curve can be considered almost as a basis for improving the seismic behavior. Figure 23 shows the hysteresis curves of the numerical and laboratory models of the samples. Improvements in the seismic behavior of the reinforced specimen were significant compared to the fabricated specimen. For example, because the specimens are loaded to their final capacity, the capacity is increased by about 20 to 25 percent, and the area under the displacement-force curve can be considered almost as a basis for improving seismic behavior. Permanent deformation is a good criterion for assessing the extent of damage, the formation of nonlinear behavior and the serviceability of structures after an earthquake.

4.4 The effect of prestressing force

To investigate the effect of prestressing force on the connection response, 3 different modes were considered. Figure 24 shows the effect of prestressing force on the connection capacity. As it is known, by increasing the

prestressing force, the connection capacity also increases. A 100% increase in the prestressing load (50kN to 100 kN) caused a 67% increase in resistance (150 kN to 250 kN), and a 1.5-fold increase (50 kN to 150 kN) in the prestressing load increased the resistance by 100% (150 kN to 300 kN).

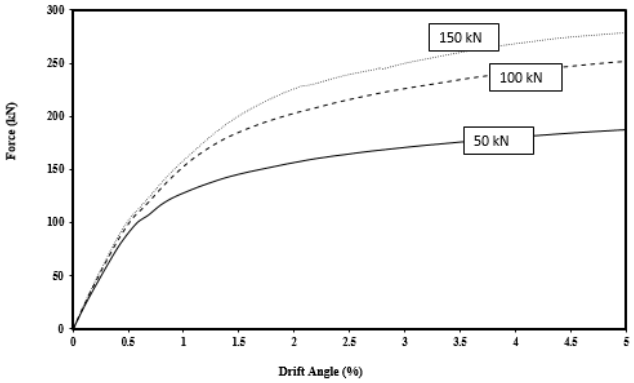

Fig. 24: Effect of prestressing force on joint capacity

4.5 Effect of FRP sheets thickness around concrete column

Because the FRP sheets of the concrete confinement provide a suitable confinement for the joint area, the thickness of the sheets was studied in 3 different sizes and its effect on connection capacity is shown in Figure 23. According to the figure, it is clear that the thickness of FRP cover sheet does not have significant effect on the final strength capacity.

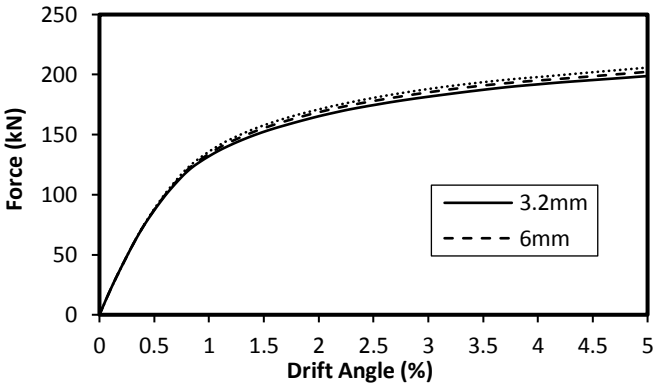

Fig. 23: Effect of FRP sheets thickness on final capacity

4. Conclusion

In this study, a sample at 30% scale under gravity and lateral cycle loading was examined in the laboratory. A finite element analysis set was used to evaluate various parameters in improving the behavior of the laboratory sample. The finite element model correctly predicted the weakness of the model, then a reinforced specimen was investigated by increasing the prestressing force in the concrete beam and the thickness of the FRP sheets used at the base of the bridge by the finite element method. The results are summarized below:

• Numerical and experimental results are consistent, exhibiting exactly the same behavior, with a maximum displacement resistance of about 2 mm, but displacements exceed this value due to cracks in the concrete in the tissue. Strength has decreased in the finite element shape. The only difference between the two diagrams is that, in the finite element model, due to the non-slip of reinforcements in concrete, the phenomenon of pinching is not seen in the finite element diagram.

• The seismic properties of the improved samples are considerably improved compared to the constructed samples. When the sample is loaded to its final capacity, increasing the capacity and area under the force-displacement curve can be considered almost the basis for improving seismic behavior.

• Cracks in concrete columns start at the joint with the beam near the load location and gradually propagate down the column as the load continues. Apparently, due to the double curvature of the cap-beam, the crack at the end connecting to the concrete column is close to where the load is applied to the cap-beam at the connection to the next column. The upper part of the concrete beam expands to the lower surface of the cap-beam and therefore by reversing, the load will reverse. Therefore, in lateral loading, the places that need reinforcement are the connection point of the column to the concrete beam and also the areas of the concrete beam that are adjacent to the column.

•Cracks formed on the surface of concrete columns do not propagate vertically to the outer surface of the concrete, but rather at a slight slope towards the joint. This is important because if the concrete columns need to be reinforced, these reinforcements will be placed in this area perpendicular to the direction of the crack. The best case is to place the hammer perpendicular to the crack.

•The stress concentration of the column reinforcements below the joint area indicates that the reinforcements in this area are heavily stressed by the load.

•Three different modes were considered to investigate the effect of prestress forces on the assembly response. As the prestressing load increases, so does the connection capacity.

References

[1] Wang, Y., Ibarra, L., & Pantelides, C. (2016). Seismic retrofit of a three-span RC bridge with buckling-restrained braces. Journal of Bridge Engineering, 21(11), 04016073.

[2] Hsu, Y., and Fu, C. (2004). "Seismic effect on highway bridges in Chi Chi Earthquake." J. Perform. Constr. Facil., 10.1061/(ASCE)0887 -3828(2004)18:1(47), 47–53.

[3] Ab e, M., and Shimamura, M. (2012). "Performance of railway bridges during the 2011 Tōhoku Earthquake." J. Perform. Constr. Facil., 10.1061/(ASCE)CF.1943-5509.0000379, 13–23.

[4] Han, Q., Qin, L., and Wang, P. (2013). "Seismic failure of typical curved RC bridges in Wenchuan Earthquake." Proc., 6th China–Japan–US Trilateral Symposium on Lifeline Earthquake Engineering, ASCE, Reston, VA, 425–432.

[5] Kwon, O., Elnashai, A. S., Gencturk, B., Kim, S., Jeong, S., and Dukes, J. (2011). "Assessment of seismic performance of structures in 2010 Chile Earthquake through field investigation and case studies." Proc., 2011 Structures Congress, ASCE, Reston, VA.

[6] Johnson, N., Ranf, R., Saiidi, M., Sanders, D., and Eberhard, M. (2008). "Seismic testing of a two-span reinforced concrete bridge." J. Bridge Eng., 10.1061/(ASCE)1084-0702(2008)13:2(173), 173–182.

[7] Priestley, M. N., Seible, F., and Calvi, G. M. (1996). Seismic design and retrofit of bridges, John Wiley and Sons, New York.

[8] Zong, Z., Xia, Z., Liu, H., Li, Y., and Huang, X. (2016). "Collapse failure of prestressed concrete continuous rigid-frame bridge under strong earthquake excitation: Testing and simulation." J. Bridge Eng., 10.1061 /(ASCE)BE.1943-5592.0000912, 04016047.

[9] Berry, M., Parrish, M., and Eberhard, M. (2004). PEER structural performance database user's manual (version 1.0), Univ. California, Berkeley, CA.

[10] Chang, S., Li, Y., and Loh, C. (2004). "Experimental study of seismic behaviors of as-built and carbon reinforced plastics repaired reinforced concrete bridge columns." J. Bridge Eng., 10.1061/(ASCE)1084 -0702(2004)9:4(391), 391–402.

[11] Cheng, C. T., Yang, J. C., Yeh, Y. K., and Chen, S. E. (2003). "Seismic performance of repaired hollow-bridge piers." Constr. Build. Mater., 17(5), 339–351.

[12] Priestley, M. N., Seible, F., Xiao, Y., and Verma, R. (1994). "Steel jacket retrofitting of reinforced concrete bridge columns for enhanced shear strength. Part 1: Theoretical considerations and test design." Struct. J., 91(4), 394–405.

[13] Priestley, M. J. N., Seible, F., and Anderson, D. L. (1993). "Proof test of a retrofit concept for the San Francisco double-deck viaducts. Part 1: Design concept, details, and model." Struct. J., 90(5), 467–479.

[14] Sritharan, S. S., Priestley, M. J. N., and Seible, F. (1999). "Enhancing seismic performance of bridge cap beam-to-column joints using prestressing." PCI J., 44(4), 74–91

[15] Pantelides, C., Gergely, J., Reaveley, L., and Volnyy, V. (1999). "Retrofit of RC bridge pier with CFRP advanced composites." J. Struct. Eng., 10 .1061/(ASCE)0733-9445(1999)125:10(1094), 1094–1099.

[16] Mander, J. B., and Chen, S. (1995). "Seismic retrofit procedures for reinforced concrete bridge piers in the eastern United States." NCEER Rep. 5, National Center for Earthquake Engineering Research, Buffalo, NY.

[17] Priestley, M. J. N., and Paulay, T. (1992). Seismic design of reinforced concrete and masonry buildings, John Wiley and Sons, New York.

[18] AASHTO. (2007). AASHTO movable highway bridge design specifications, Washington, DC.

[19] Bahrani, M. K., Vasseghi, A., Esmaeily, A., and Soltani, M. (2010). "Experimental study on seismic behavior of deficient conventional bridge bents." J. Seismol. Earthquake Eng., 12(3).

[20] Barr P J, Stanton J F, Eberhard M O. Effects of temperature variations on precast, prestressed concrete bridge girders. J. Bridge Eng. 2005; 10(2): 186-194.
DOI: https://doi.org/10.1016/0045-7825(79)90027-6

[21] Pan Z, Fu C C, Jiang Y. Uncertainty analysis of creep and shrinkage effects in long-span continuous rigid frame of Sutong Bridge. J. Bridge Eng. 2010; 16(2): 248-258.
DOI：http://doi.org/10.1109/ICETCE.2011.5774695

[22] Jung K H, Yi J W, Kim J H J. Structural safety and serviceability evaluations of prestressed concrete hybrid bridge girders with corrugated or steel truss web members. Eng. Struct. 2010; 32(12): 3866-3878.
DOI：http://doi.org/10.1016/j.engstruct.2010.08.029

[23] Malm R, Sundquist H. Time-dependent analyses of segmentally constructed balanced cantilever bridges. Eng. Struct. 2010; 32(4): 1038-1045.

DOI: https://doi.org/10.1016/j.engstruct.2009.12.030

[24] El-Ariss B. Behavior of beams with dowel action. Eng. Struct. 2007; 29(6): 899-903.
DOI: https://doi.org/10.1016/j.engstruct.2006.07.008

[25] Podolny W J. The cause of cracking in post tensioned concrete box girder bridges and retrofit procedures. PCI J. 1985; 30(2): 82–139.
DOI: http://doi.org/10.15554/pcij.03011985.82.139

[26] Wei L, Sheng X, Xiao R. Mechanism and prevention countermeasures of cracking for bottom slab in a continuous prestressed concrete box girder. Struct. Eng. 2007; 23(2): 53–57.DOI: http://doi.org/10.1177/1369433218815436

[27] Megally S, SEIBLE F, GARG M, et al. Seismic performance of precast segmental bridge superstructures with internally bonded prestressing tendons. PCI J. 2002; 47(2): 40-56.DOI: 10.15554/pcij.03012002.40.56

[28] Sennah K M, Kennedy J B. State-of-the-art in design of curved box-girder bridges. J. Bridge Eng. 2001; 6(3): 159-167.DOI：https://doi.org/10.1061/(ASCE)1084-0702(2001)6:3(159)

[29] Ataei N, Padgett J E. Limit state capacities for global performance assessment of bridges exposed to hurricane surge and wave. Struct. Saf. 2013; 41: 73-81.
DOI: https://doi.org/10.1016/j.strusafe.2012.10.005

[30] JTG D62-2004. Design Code for Design of Highway Reinforced Concrete and Pre-stressed Concrete Bridge Culvert. 2004.

[31] Wu H Q, Gilbert R I. Modeling short-term tension stiffening in reinforced concrete prisms using a continuum-based finite element model. Eng. Struct. 2009; 31(10): 2380-2391.DOI: https://doi.org/10.1016/j.engstruct.2009.05.012

[32] Zhou S J. Finite beam element considering shear-lag effect in box girder. J. Eng. Mech. 2010; 136(9): 1115-1122.DOI: http://doi.org/10.1260/1369-4332.18.6.817

[33] Lou T, Lopes S M R, Lopes A V. A finite element model to simulate long-term behavior of prestressed concrete girders. Finite Elem. Anal. Des. 2014; 81: 48-56.
DOI：https://doi.org/10.1016/j.finel.2013.11.007

[34] Pedziwiatr J. The influence of the bond between concrete and reinforcement on tension stiffening effect. Mag. Concrete Res. 2009; 61(6): 437-443.
DOI: http://doi.org/10.1680/macr.2008.00097

[35] Pimentel M, Figueiras J. Assessment of an existing fully prestressed box-girder bridge. Proceedings of the Institution of Civil Engineers-Bridge Engineering. Thomas Telford Ltd 2015; 1-12.DOI: http://doi.org/10.1680/jbren.15.00014

[36] Chen L, Tang G B. Influence of Longitudinal Cracks in Bottom Flange of Concrete Continuous Box Girder. Appl. Mech. Mater. 2015; 744: 773-778.
DOI: http://doi.org/10.4028/www.scientific.net/AMM.744-746.773

[37] Al-Manaseer A A, Phillips D V. Numerical study of some post-cracking material parameters affecting nonlinear solutions in RC deep beams. Canadian J. Civ. Eng. 1987; 14(5): 655-666.
DOI: https://doi.org/10.1139/l87-096

[38] Wang, G., Ding, Y., & Liu, X. The monitoring of temperature differences between steel truss members in long-span truss bridges compared with bridge design codes. Advances in Structural Engineering, 2019; 22(6): 1453–1466.
DOI: http://doi.org/10.1177/1369433218815436

[39] Yuan, M., Liu, Y., Yan, D., & Liu, Y. Probabilistic fatigue life prediction for concrete bridges using Bayesian inference. Advances in Structural Engineering, 2019; 22(3): 765–778.
DOI: http://doi.org/10.1177/1369433218799545

[40] X. H. Zhang, W. Zhang, Y. M. Luo, et al., Interface Shear Strength between Self-Compacting Concrete and Carbonated Concrete American Society of Civil Engineers, 2018; 32(6):04020113. DOI: https://doi.org/1061/(ASCE)MT.1943-5533.00032

[41] E. Gottsäter, M. Johansson, M. Plos, Ivanov O. Larsson Crack widths in base restrained walls subjected to restraint loading Eng Struct, 189 (2019), pp. 272-285, 10.1016/j.engstruct.2019.03.089

[42] E. Gottsäter, O. Larsson Ivanov, M. Molnár, R. Crocetti, F. Nilenius, M. Plos Simulation of thermal load distribution in portal frame bridges Eng Struct, 143 (2017), pp. 219-231, 10.1016/j.engstruct.2017.04.012

[43] Zandi K, Ransom EH, Topac T, Chen R, Beniwal S, Blomfors M, et al. A Framework For Digital Twin of Civil Infrastructure - Challenges and Opportunities. 12th Int. Work. Struct. Heal. Monit. Stanford, California, USA, Sept. 10-12, 2019, Lancaster, PA, USA: DEStech Publications, Inc.; 2019, p. 7 pp.

[44] I.H. Kim, H. Jeon, S.C. Baek, W.H. Hong, H.J. Jung Application of crack identification techniques for an aging concrete bridge inspection using an unmanned aerial vehicle Sensors, 18 (2018), pp. 1-14, 10.3390/s18061881

[45] C.G. Berrocal, I. Fernandez, R. Rempling Crack monitoring in reinforced concrete beams by distributed optical fiber sensors Struct Infrastruct Eng (2020), pp. 1-16, 10.1080/15732479.2020.1731558

[46] ABAQUS standard user's manual, version 6.18.